Code Comparison for the Assessment of Masonry Capacity

Mir Abdul Kuddus[1*], Pere Roca Fabregat[2]

[1]*Assistant Professor, Department of Civil Engineering, Khulna University of Engineering &Technology, Khulna-9203, Bangladesh*

[2]*Professor, Department of Civil and Construction Engineering, Technical University of Catalonia, Barcelona-08034, Spain*

ABSTRACT: *Masonry load bearing wall subjected to vertical concentric and eccentric loading may collapse through instability. In this Paper the buckling behavior of masonry load bearing wall of different slenderness ratio were investigated via testing a series of scale masonry wall subjected to concentric and eccentric vertical loading. A total of thirty six masonry walls were tested in the Laboratory of Technical University of Catalonia (UPC), which was the basis of the numerical study. A numerical finite element model was developed based on the simplified micro model approach and calibrated by using those results found from experimental study. The influence of nonlinear behavior of interface element, slenderness ratio and various end conditions have been investigated together with the effect of different end eccentricity of vertical load. However, a series of analytical studies were conducted in order to access the accuracy and performance of formulations provided by EUROCODE 6 and ACI-530 for vertical capacity of masonry wall.*

Keywords: *Masonry load bearing wall, buckling failure, eccentric load, slenderness ratio, micro-modeling.*

I.   INTRODUCTION

The buckling response of masonry walls depends on parameters such as the cross-sectional area, the material properties, the slenderness and the effective eccentricities of loads at each end of the element. In masonry design standards, these factors are treated in different ways. For example, the north-American ACI-530 code and the European EUROCODE-6 (EC-6) show significant differences in the analysis of brickwork walls under eccentric axial load. Whereas ACI-530 code analyzes the buckling failure and the cross-section material failure separately, EC-6 deals with both failure modes in a single analytical formulation.

The literature on the subject shows large number of studies carried out on axially loaded walls with varying slenderness ratio. Among the first, Chapman and Slatford (1957) obtained closed form solutions for the load deformation behaviour of brittle elastic wall by assuming that masonry material has no tensile strength and that cracking occurs whenever a tensile stress would develop. After that Yokel's (1971) results on the buckling of walls made of no-tension material are well known. De Falco's proposal (2002) on the stability of columns using an elastic-plastic material model stands among the most recently presented analytical approaches. More recently, Mura (2008) has utilized a parabolic stress-strain relationship to describe the behaviour of the brickwork under compression loads. Shalin (1978) reviewed the results of analysis carried out by a number of authors and presented experimental evidence in support of the calculations.

Further work was carried out by Sawko and Towler (1982) who proposed a numerical procedure for calculating the failure load of a no-tension material wall. An analytical solution has been carried out by Romano et al. (1993), considering no tension bearing masonry with a monomial stress–strain relationship in compression. Parland et al. (1982) proposed a method for determining buckling failure load of a slender wall, taking into account the effect of tension stress field which exists between the cracked joints. However, the linear elastic materials were used in this analysis.

The micro-modelling strategy has been adopted in the present research in order to carry out the needed numerical simulations. The prediction of the ultimate capacity of walls obtained by means of micro-modelling approach compared with experimental and analytical results. Moreover, results obtained in the parametric studies by considering different end support condition and effect of support codition on failure loads of walls were investigated. Conclusions are drawn on the relative importance of end support condition, non-linear geometrical and material properties with different end eccentricity.

II.   LABORATORY INVESTIGATION

This chapter deals with the description of the testing program carried out in Structural Technology Laboratory of the Technical University of Catalonia which was the basis of numerical simulation of this research. The following is the characterization of materials used for the manufacture of the walls and a description of the manufacturing process, with emphasis on those details because it is a 1:4 scale study. Thirty six walls were tested with slenderness ratio (calculated as h / t) 6, 12, 18 and 25 and values of eccentricity of load was e = 0, e =t/6 and e = t/3. A summary of the number and type of the test specimens and test program is shown in Table 1.

Table 1: Summary of number and type of test specimens.

Wall series	Slenderness ratio	Height (cm)	Eccentricity of load	Support condition	Observation
W-0-6	6	21	0	Hinge-hinge	Slenderness ratio calculated as H/t
W-0-12	12	42	0		
W-0-18	18	63	0		
W-0-25	25	87.5	0		
W-1/6-6	6	21	t/6	Hinge-hinge	Slenderness ratio calculated as H/t
W-1/6-12	12	42	t/6		
W-1/6-18	18	63	t/6		
W-1/6-25	25	87.5	t/6		
W-1/3-6	6	21	t/3	Hinge-hinge	Slenderness ratio calculated as H/t
W-1/3-12	12	42	t/3		
W-1/3-18	18	63	t/3		
W-1/3-25	25	87.5	t/3		

The walls were constructed as single leaf with scale of 1:4. The width was of 297 mm and thickness of 35 mm. In order to introduce different slenderness ratio, walls were built with heights of 210 mm, 420 mm, 630 mm and 875 mm. The thickness of the vertical and horizontal joints was approximately 2.5 mm. Figure 1 shows the layout of the tested wall. One fourth scale bricks were used for the construction of walls. The dimensions of the bricks (Length x width x thickness) are 72.5 x 35 x 12.5 mm. The average density of the brick was found, 1717.17 kg/m^3, after the drying process. The compressive strength of the brick is f_b = 32.45 MPa. The mortar used for the construction of the masonry walls was an M-8 prepared mortar. In order to adjust the fineness of the mortar for 1:4 scale sieving is made of it, removing all the percentage of material retained by the sieve1 mm aperture, since the presence of larger sizes difficult to maintain size of the joint.
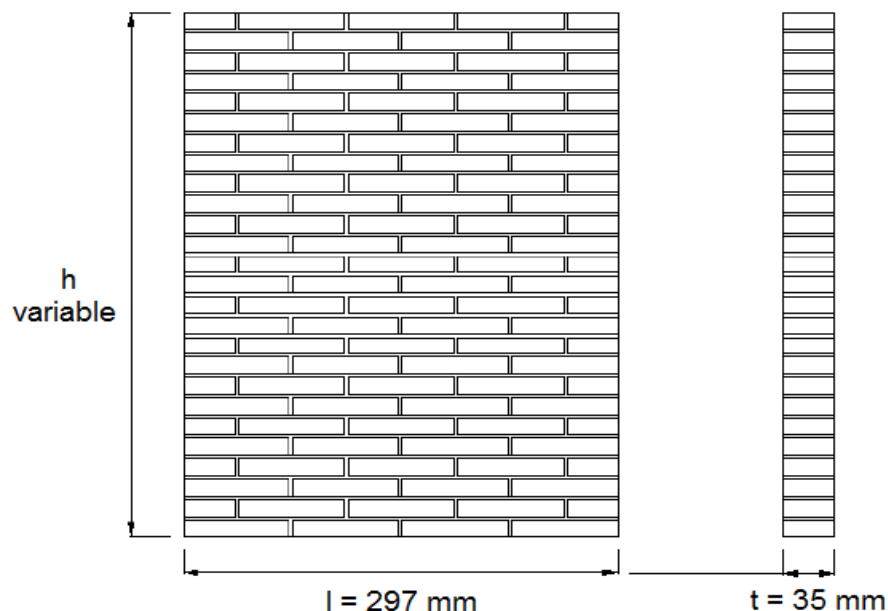
Figure 1: Layout of tested wall.

The average value of flexural strength is 3.05 MPa and the average compressive strength of the mortar is 7.29 MPa which was taken as the value for the further calculation. To determine the uniaxial compression and Young's modulus of elasticity five specimens of 147.5 mm x 147.5 mm (height of 10 rows and width of 2 pieces) considered. The average value of the compressive strength and Young's modulus obtained from the test are 14.2 MPa and 3458 MPa respectively.

III.   ADOPTED MODELING STRATEGY

The numerical simulation presented is performed with the well-known micro-model proposed by Lourenco & Rots (1997) requires more specific software oriented to masonry analysis. For all cases, micro-models assume 2D plain-stress and a hinged-hinged configuration. The hinges are modeled by means of stiff triangular objects placed at the bottom and at top of the wall, whose end vertex is allowed to freely rotate. In addition, a minimum eccentricity of 1mm is always applied in order to account for possible irregularities of the wall geometry of the load positioning. Basically, the model assigns an elastic behavior to the units whereas masonry inelastic behavior is transferred to the joints. This analysis was performed with DIANA software. The integration schemes used are 2x2 points Gauss integration for the continuum elements and 3 points Lobato integration for the interface elements. An interface allows discontinuities in the displacement field and its behavior is described in terms of a relation between the traction t and relative displacement u across the interface. In the multisurface interface model for the masonry proposed by Lourenco and Rots, the quantity of traction and displacement is denoted as generalized stress σ and generalized strain, ε. In this case the elastic constitutive relation between stresses and strain is given by:
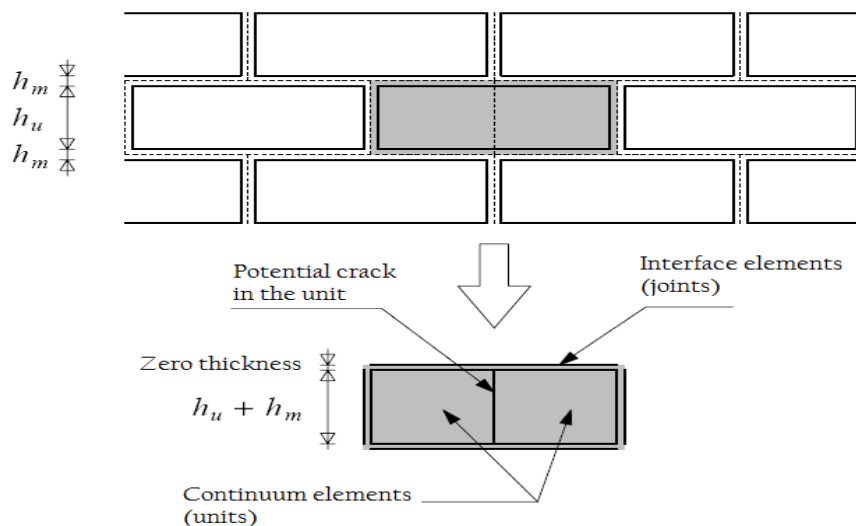
$$\sigma = D\varepsilon \qquad\qquad (1)$$

For 2D configuration $D = diag\{k_n, k_s\}, \sigma = (\sigma, \tau)^\tau and \varepsilon = (u_n, u_s)$

Where, n and s is the normal and shear components respectively. The terms in the elastic stiffness matrix can be obtained from the properties of both masonry components and thickness of the joint as:

$$k_n = \frac{E_u E_m}{t_m(E_u - E_m)}; k_s = \frac{G_u G_m}{t_m(G_u - G_m)} \qquad\qquad (2)$$

Where, E_u and E_m = Young's moduli; G_u and G_m = Shear moduli and t_m = thickness of the joint.

Figure 2: Proposed modeling strategy.

The interface model includes a compressive cap where the complete inelastic behavior of masonry in compression is lumped. This is a phenomenological representation of masonry crushing because the failure process in compression explained by the microstructure of units and mortar and the interaction between them. In the model the failure mechanism represented in such way that the global stress strain diagram is captured. The model was justified by Lobato et al. and found that the model is efficiently able to reproduce the experimental results. For this reason, the proposed micro-model was selected by the author to simulate the wall for buckling failure.

IV.   MODEL DESCRIPTION

In the numerical simulation, the units were modelled by using plain-stress continuum 8-node elements and for the mortar joints adopted 6-node zero-thickness line interface elements. In addition, hinges are modelled by means of stiff triangular objects. Each unit was modelled with 12 x 3 elements. The geometry and meshing of the wall for slenderness ratio 6 and eccentricity 0, t/6 and t/3 are shown in the Figure 3. For all cases, micro-models of wall considered hinged-hinged configuration. The vertical load was applied concentrically and eccentrically as unit deformation. The boundary condition and loading configuration is also shown in the Figure 3.
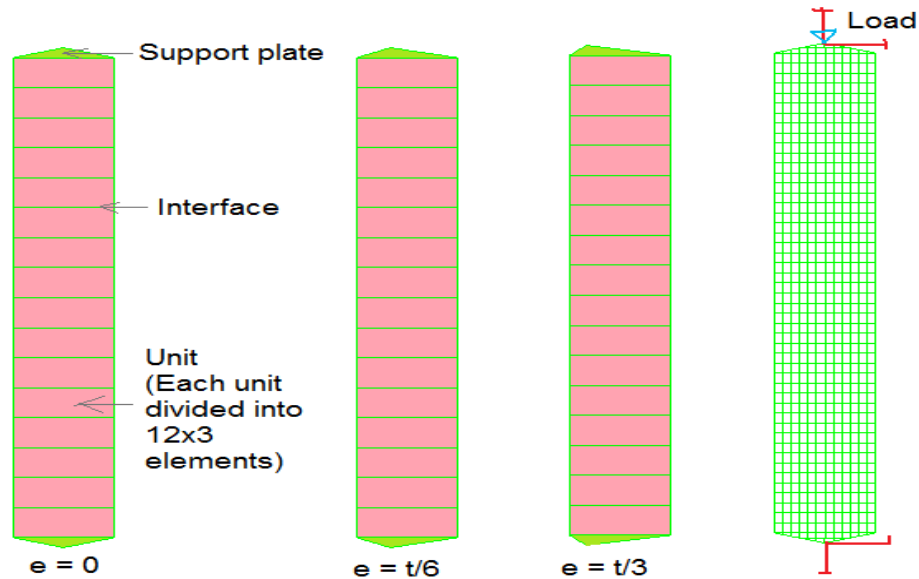
Figure 3: Geometry, Meshing and Load of wall for slenderness ratio 6.

4.1 Material Properties

The material parameters used for the numerical simulation are shown in the Table 2. Some parameters such as $G^I{}_f$ and C_S have been taken directly from the previous research. The fracture energy for mode I, $G^I{}_f$ have been taken from the test carried out by Van der Pluijm (1992) and for the parameter of shape of elliptical cap C_S a value of 9 has been adopted from Lourenco (1996). The interface elastic stiffness values were calculated from thickness of the joint h_j, the Young's moduli of unit and joint E_u and E_j, respectively, and the shear moduli of unit and joint G_u and G_j, respectively as CUR (1994):

$$k_n = \frac{E_u E_j}{h_j(E_u - E_j)}; k_t = \frac{G_u G_j}{h_j(G_u - G_j)} \tag{3}$$

The different strength values f_f, c and f_m have been obtained from the experimental study carried out in UPC (2010). The compressive fracture energy G_{fc} and equivalent relative displacement k_p calculated according to Model Code 90 and Eurocode 6, respectively by using followings formula (Lourenco, 1996):

$$G_{fc} = 15 + 0.43 f_m - 0.0036 f_m{}^2; k_p = \{0.002 - f_m(\frac{1}{E_u} + \frac{1}{k_n(h_u + h_j)})\} \tag{4}$$

Table 2: Material parameters adopted for numerical analysis.

Components	Parameter	Symbol	Units	Values
Brick	Elastic modulus	E_b	N/mm^2	4800
	Poison ratio	v	-	0.15
	Tensile strength	f_{tb}	N/mm^2	3.95
Joint	Normal stiffness	k_n	N/mm^2	2800
	Shear stiffness	k_t	N/mm^2	1900
	Bond tensile strength	f_t	N/mm^2	0.554
	Mode – I fracture energy	$G^I{}_f$	Nmm/mm^2	0.02
	Cohesion	c	-	0.45
	Mode – II fracture energy	$G^{II}{}_f$	Nmm/mm^2	0.175
	Angle of internal friction	$tan\varphi$	-	0.812
	Angle of dilatancy	$tan\Psi$	-	0.009
	Compressive strength of masonry	f_m	N/mm^2	14.20
	Compressive fracture energy	G_{fc}	Nmm/mm^2	20.38

4.2 Validation of Model

The micro-models were validated next by a comparison with experimental results obtained from UPC (2010). The main concern of this work was, to demonstrate the ability of the model to capture the behaviour observed in the experiments and close quantitative reproduction of the experimental results.
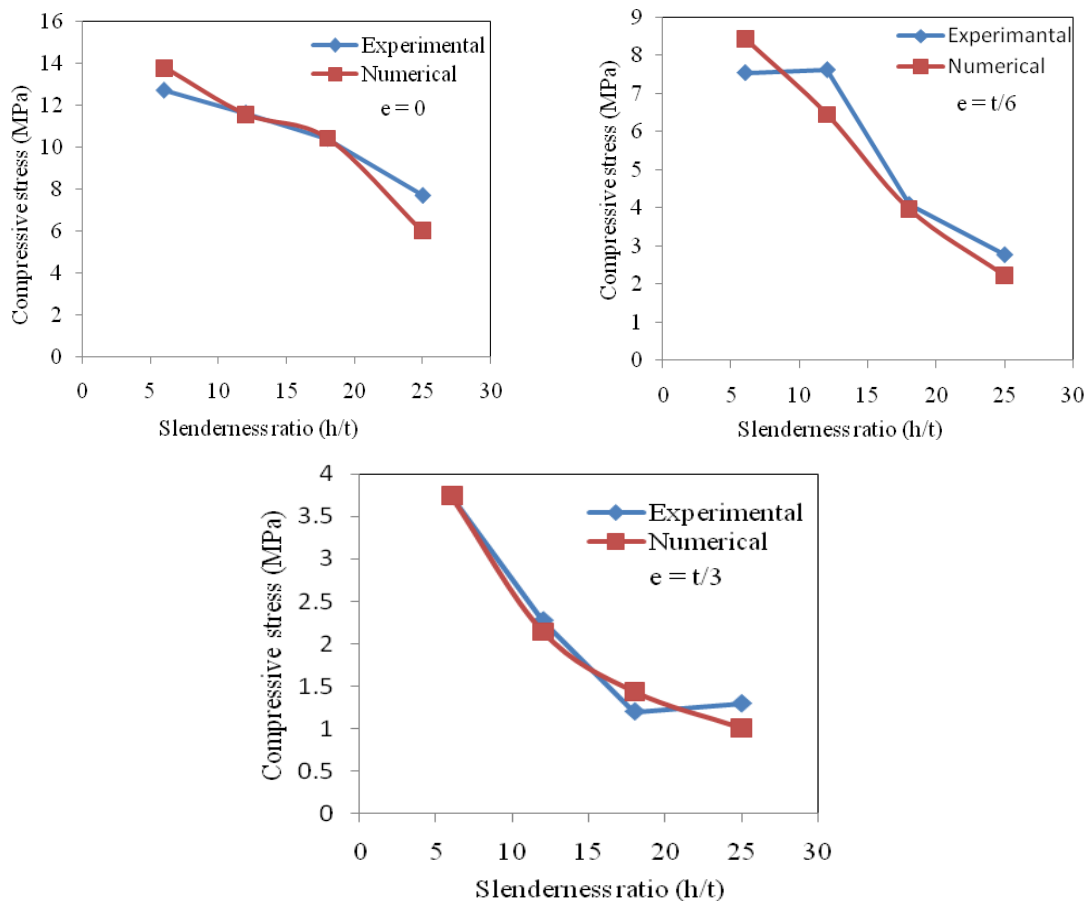
Figure 4: Comparison of compressive stress for different load eccentricity.

The comparison between the experimental collapse load and collapse load obtained from the micro-model is presented in the Figure 4. The figures shows that the experimental behavior is satisfactorily reproduced and the collapse load estimated within a 15 % range of the experimental values. The micro-modeling approach is being able to provide a very satisfactory estimation of the experimental capacity of the walls particularly, for the case with e = 0. The average errors are 7.85%, 12.6% and 11.93% for the eccentricity of 0, t/6 and t/3 respectively. For all cases, one tendency is clear that with the increasing of slenderness ratio and application of load eccentricity the capacity of the wall decreased.

V. ANALYTICAL APPROACH

5.1   Eurocode 6 (EC 6)

According to Eurocode-6, the resistance of a masonry wall subjected to vertical load depends on the geometry of the wall, the eccentricities of the load and constituent material properties. This development allowed the following assumptions:

- After each cross-section deformation remains plane and normal to the deformed axis (Bernoulli-Navier hypothesis);
- The resistance of the wall in tension perpendicular to the bed joints is zero.

5.1.1   Determination of Vertical Load Resistance

The vertical load resistance of a single leaf wall per unit length, N_{RD}, can be calculated as:

$$N_{RD} = \frac{\Phi_{i,m} t f_k}{\gamma_M} \qquad\qquad (5)$$

Where, $\Phi_{i,m}$ is the capacity reduction factor Φ_i (top or bottom of wall) or Φ_m (in the middle one fifth of the height of wall), allowing for the effects of slenderness and eccentricity of loading, f_k is the characteristic compressive strength of masonry according to paragraph 3.6.2 of EC 6, if the cross-sectional area

A is less than 1 m², this property is multiplied by the factor (0.7 + 3A), γ_M is the partial safety factor for the material, under paragraph 2.3.3.2 of EC 6 and t is the thickness of the wall, taking into account the depth of recesses in joints greater than 5 mm.

5.1.2 Determination of Reduction Factor for Slenderness ratio and Eccentricity
- At the top or bottom of the wall.

$$\Phi_i = 1 - \frac{2e_i}{t} \qquad\qquad (6)$$

Where, e_i is the eccentricity at the top or the bottom of the wall;

$$e_i = \frac{M_i}{N_i} + e_{hi} + e_a \ge 0.05t$$

M_i is the design bending moment at the top or the bottom of the wall resulting from the eccentricity of the floor load at the support, according to 4.4.7 (Figure 4.1) of EC 6;

N_i is the design vertical load at the top or bottom of the wall;

e_{hi} is the eccentricity at the top or bottom of the wall, if any, resulting from horizontal loads (for example, wind);

$e_a = \dfrac{h_{ef}}{450}$; is the accidental eccentricity and

t is the thickness of the wall.

- In the middle one fifth of the wall height.

$$\Phi_m = A_1 e^{\left(-\frac{u^2}{2}\right)} \qquad\qquad (7)$$

Where, A_1 Numerical factor, $A_1 = 1 - 2\dfrac{e_{mk}}{t}$

u is the Numerical factor, $u = \dfrac{\left(\dfrac{h_{ef}}{t_{ef}} - 2\right)}{23 - 37\dfrac{e_{mk}}{t}}$

h_{ef} is the effective height, obtained from 4.4.4 of EC 6 for the appropriate restraint or stiffening condition;

t is the thickness of the wall;

t_{ef} effective thickness of the wall in accordance with paragraph 4.4.5 of the EC 6;

e is the base of natural logarithms, approximately, e = 2.71828;

e_{mk} is the eccentricity within the middle one fifth of the wall height;

$$e_{mk} = e_m + e_k \ge 0.05t$$

with $e_m = \dfrac{M_m}{N_m} + e_{hm} \pm e_a$

e_m is the eccentricity due to loads;

M_m is the greatest moment within the middle one fifth of the height of the wall resulting from the moments at the top and bottom of the wall, see Figure 6 (a);

N_m is the design vertical load within the middle one fifth of the height of the wall;

e_{hm} is the eccentricity at mid-height resulting from horizontal loads (for example, wind);

e_k is the eccentricity due to creep;

$$e_m = 0.002\Phi_\infty \frac{h_{ef}}{t_{ef}}\sqrt{te_m}$$

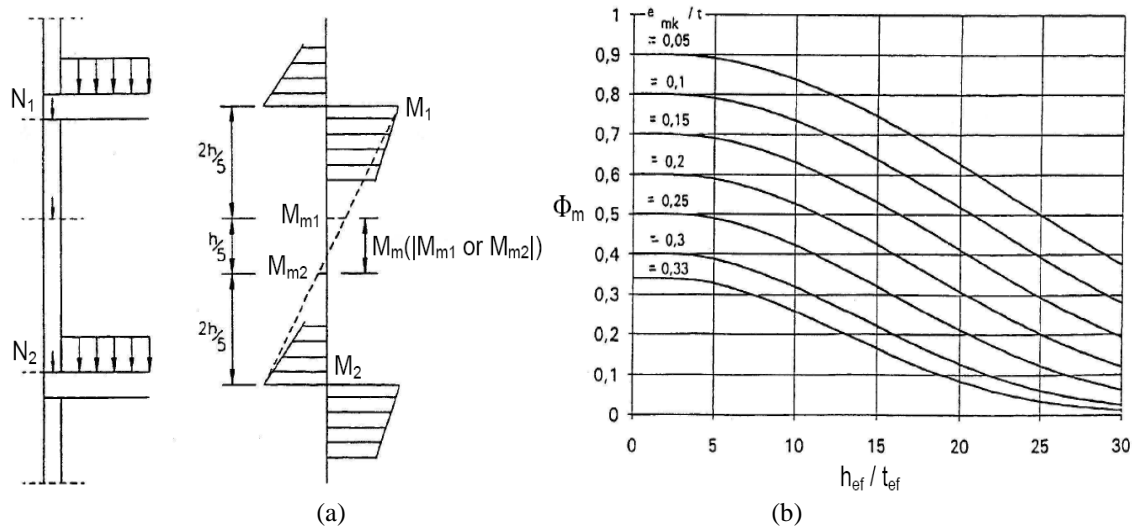Φ_{∞} is the final creep coefficient from Table 3.8 of EC 6.

Figure 6: (a) Moment according to EC 6 and **(b)** values of Φ_m against slenderness ratio for different eccentricity.

This development has taken a modulus of the elasticity of masonry as a thousand times the compressive resistance property of masonry ($E = 1000 f_k$).

5.2 ACI-530

ACI-530-05 code was reported by Masonry Standards Joint Committee (MSJC), the design of unreinforced masonry has included a limit on the allowable axial compression force that may be applied. The limit is that the maximum allowable compressive force P is not exceed one fourth of the buckling load P_e as defined in the code. The maximum compressive force is limited to:

$$P \le \frac{P_e}{4} \tag{8}$$

Where,

$$P_e = \pi^2 \frac{E_m I}{h^2} \left(1 - 0.577 \frac{e}{r}\right)^3 \tag{9}$$

In which, E_m = modulus of elasticity; I = uncracked moment of inertia of the section; e = eccentricity of the compressive force P; r = radius of gyration of the uncracked unit section; h = unbraced height of the member under load. As the member deflects and bends under the action of eccentrically applied force, flexural tension cracking occur wherever the bending stress due to moment exceed the axial compression stress. The buckling equations for members subjected to compressive force are shown below:

$$P_e = \pi^2 \frac{E_m I}{h^2} \left(1 - 2\frac{e}{t}\right)^3 \tag{10}$$

For a solid rectangular cross-section, the radius of gyration is approximately equal to $0.289t$. For members having an slenderness ratio less than 99 and greater than 99, the allowable compression stress under axial load F_a is given from the following equation 11 and 12, respectively:

$$F_a = \left(\frac{1}{4}\right) f_m \left(\frac{h}{140rh}\right)^2 \tag{11}$$

$$F_a = \left(\frac{1}{4}\right) f_m \left(\frac{70r}{h}\right)^2 \tag{12}$$

Where, f_m = specified compressive strength of masonry, t = thickness of the wall.

VI. COMPARISON OF COLLAPSE LOADS

A comparison between the experimental results obtained, the results calculated with standards ACI-530 and EUROCODE 6 (EC 6) and the proposed numerical micro-models is presented in Figure 7. As can be observed, the method proposed in EC 6 underestimates substantially the bearing capacity of the walls. The other standard considered, ACI-530, also underestimates the strength of walls in all cases.

ACI-530 code produce average error of 76.86%, 87.62% and 96.26% compared to experimental results for the cases of load eccentricity 0, t/6 and t/3 respectively. For overall cases this code shows average error 86.92%. EC 6 underestimates the strength of the walls in all cases, although it is able to reproduce the general tendency. This code provides more satisfactory estimations of collapse loads for the lower eccentricity and lower slenderness ratio specifically, for the eccentricity t/6 which provides average error of 23.94%. Moreover, EC 6 is the most conservative method to predict the collapse load of the higher eccentrically loaded walls (e=t/3) with an average error of 53.6% while it produce overall average error of 34% when compared with experimental results.
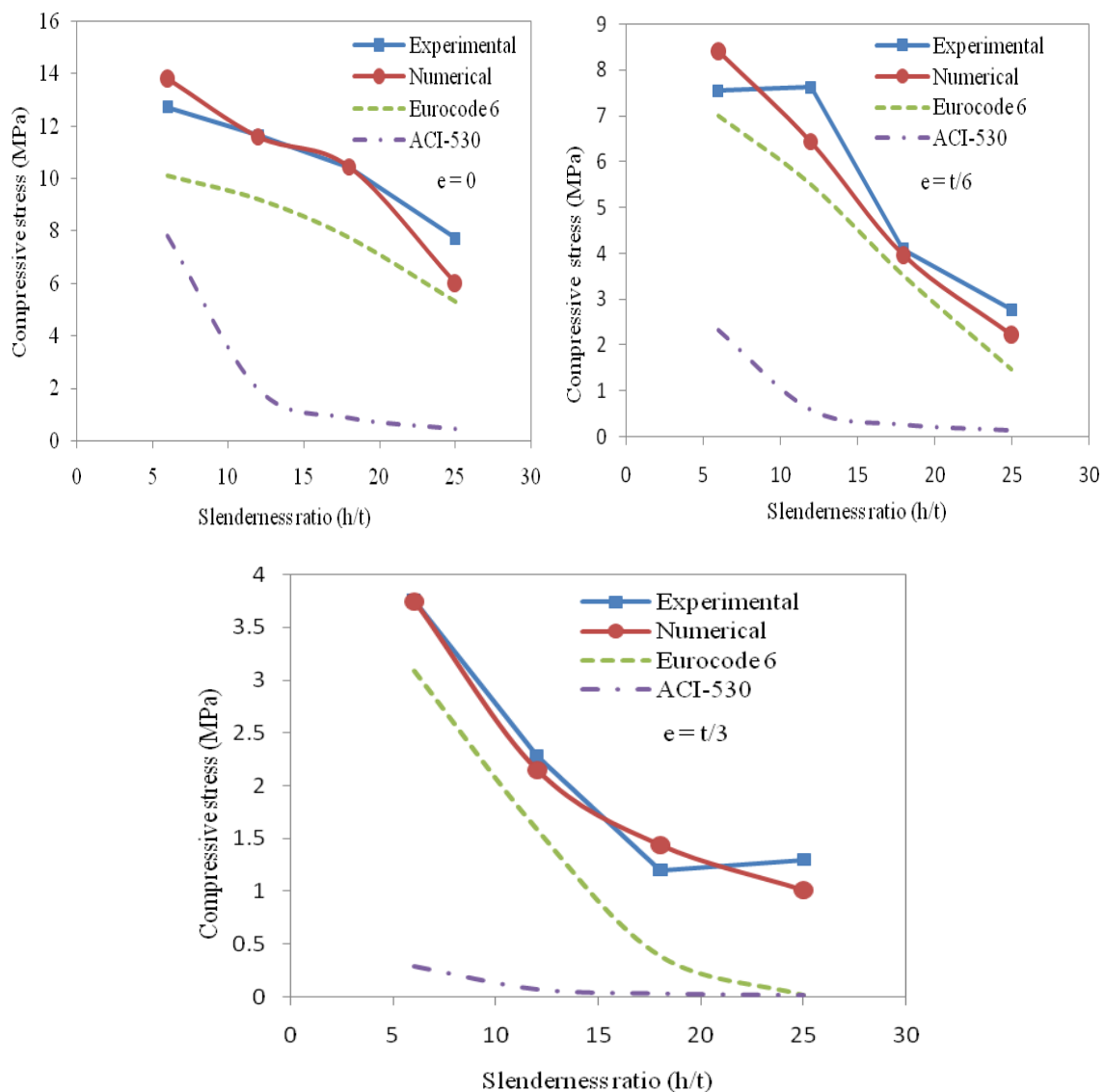
Figure 7: Comparison of compressive stress for different slenderness ratio and eccentricity.

The best fit occurs in the EC 6 (7.29%) and ACI-530 (38.47%) for the eccentricity t/6 and 0 respectively, with slenderness ratio 6 for both, while the bothe standards produce maximum error of 98.70% and 98.77% for eccentricity t/3 and slenderness ratio 25. On the other hand, both standards are underestimates the collapse load of wall when compared to numerical micro-models. ACI-530 provides most conservative results with average error of 87.19%, while EC 6 estimates collapse load by 31.30% of average error.

VII. CONCLUSIONS

The diverse combinations of slenderness ratio and load eccentricity used in the experimental program which provided the means for a comprehensive numerical analysis of the masonry wall. The micro-models afford a satisfactory prediction of the ultimate load of walls taking into account the buckling behavior. Simulations carried out by the micro-model provide the best fits for all load eccentricity, (with an average error of 10.79%). It must be noted that some difference with respect to the experimental results is unavoidable because of the influence of possible non-reported accidental eccentricities. In the case of fixed support, the load capacity increased 2 to 6 times higher than hinge support depending on slenderness ratio and eccentricity. The capacity of wall for hinge-fixed support lies between the both end hinge and both end fixed support. In the case of hinge-hinge support with high eccentricity.

The comparison between experimental and the standards' results shows significant errors of 86.92% and 34.07% for ACI-530 and EC 6, respectively. In particular, this comparison suggests that the both method proposed by EC 6 and ACI-530 tends to conservatively underestimate the strength of walls. The micro-modeling approach has shown its ability to assess the bearing capacity of masonry walls subjected to concentric or eccentric vertical loading. It has been observed that an accurate description of tensile cracking and opening of mortar joints, by means of an appropriate interface element, is essential to obtain reliable results on the bucking failure of walls.

ACKNOWLEDGEMENTS

REFERENCES

[1]. ACI-530 (2008). "ACI Manual of Concrete Practice." ACI 530.1-05/ASCE 6-05/TMS 602-05. American Concrete Institute.
[2]. CEN (1995). "Eurocode 6: Design of Masonry Structures " ENV 1996-1-1:1995, CEN, Brussels, Belgium.
[3]. Chapman, J. C. and Slatford, J. (1957). "The Elastic Buckling of Brittle Columns." Inst. Civ. Eng., Vol. 107, No. 6.
[4]. De Falco, A. and Lucchesi, M. (2007). "No Tension Beam-Columns with Bounded Compressive Strength and Deformability Undergoing Eccentric Vertical Loads." International Journal of Mechanical Sciences 49, p. 54-74.
[5]. Hasan, S. S. and Hendry, A.W. (1976). "Effect of Slenderness and Eccentricity on the Compressive Strength of Walls." Proc. 4th International Brick Masonry Conference (Brugge). Paper 4.d3.
[6]. Lourenco, P. B. (1996). "Computational Strategies for Masonry Structures." PhD thesis, Delft University of Technology, Delft, The Netherlands.
[7]. Lourenco, P. B. and Rots, J.G (1997). "Multisurface Interface Model for Analysis of Masonry Structures." Journal of engineering mechanics, 123(7), p. 660-668.
[8]. Lourenco, P. B. (1996). "A User / Programmer Guide for the Micro-modeling of Masonry Structures." TU- DELFT, Report no. 03-21-1-31-35, Delft University of Technology, Delft, The Netherlands.
[9]. Mura, I. (2008). "Stability of Nonlinear Masonry Members Under Combined Load." Computers and Structures 86, p. 1579-1593.
[10]. Page, A.W. (1978). "Finite Element Model for Masonry." J. Struc. Div., ASCE, 104(8), p. 1267-1285.
[11]. Parland, H. (1982). "Basic Principles of the Structural Mechanics of Masonry: A Historical Review." Int. J. Mas. Constr., 2(2).
[12]. Payne, D. C., Brooks, D. S. and Dved, G. (1990). "The Analysis and Design of Slender Brick Walls." Masonry International Journal, 4(2), p. 55-65.
[13]. Pluijm, R. V (1992). "Material Properties of Masonry and its Components Under Tension and Shear." Proc. 6th Canadian Masonry Symposium, Eds. V.V. Neis, Saskatoon, Saskatchewan, Canada, p. 675-686.
[14]. Sahlin, S. (1978). "Structural Masonry." Prentice-Hall Inc., New jersey, U. S. A.
[15]. Sawko, F. and Towler, F. (1982). "Numerical Analysis of Walls and Piers with Different End Conditions." 6IBMAC. Ed. Laterconsult s.v.l., Rome, Italy.
[16]. TNO DIANA (2010). "Finite Element Analysis." The Netherlands.
[17]. Valladares, I. N. (2010). "Estudi Experimental de la Fallada a Vinclament de Parets de Càrrega de Fábrica de Maó." MSc. thesis, Technical University of Catalonia, Barcelona, Spain.
[18]. Yokel, F. Y. (1971). "Stability and Load Capacity of Members with no Tensile Strength." J. Struct. Div. ASCE, 97(7), p. 1913-1926.